DOI: 10.17344/acsi.2024.9095 *Acta Chim. Slov.* **2025,** *72,* 133–144

Scientific paper

Manganese, Cobalt, Nickel and Zinc Complexes with Pyrazine-2-carboxylic Acid

Saša Petriček

Faculty of Chemistry and Chemical Technology, University of Ljubljana, Večna pot 113, 1000 Ljubljana

** Corresponding author: E-mail: sasa.petricek@fkkt.uni-lj.si*

Received: 12-02-2024

Abstract

New complexes of zinc (**1**), manganese(II) (**2** and **2a**), cobalt(II) (**3**) and nickel(II) chloride (**4**), with pyzaH (pyrazine-2-carboxylic acid) were synthesized. The pyzaH molecules are coordinated as monodentate ligands only through heterocyclic nitrogen in **1**, **2** and **3**, as shown by single crystal X-ray diffraction analysis. The chloride ions are coordinated as terminal ligands in **1**, $[ZnCl_2(pyzaH)_2]\cdot 2H_2O$, but act as bridging ligands in the 1D complexes $[MCl_2(pyzaH)_2]_n\cdot 2nH_2O$ (M = Mn, **2**, Co, **3**). The supramolecular architectures of the complexes differ due to the coordination of the chlorides, the hydrogen bonds and the parallel stacking arrangements of the pyzaH molecules. In contrast to the isolated crystals of **1**, **2** and **3**, the manganese(II) (**2a**) and nickel(II) (**4**), compounds do not contain water. According to the IR spectra and the results of thermal analyzes, the proposed formula is $[MCl_2(pyzaH)_2]$. Powder X-ray and thermal analysis results demonstrate the isostructural nature of complexes **2a** and **4**. The low thermal stability of **1** is due to the monodentate coordination of pyzaH in **1**. Thermal decomposition of **1**, **2a** and **4** in air produces oxides MO (M = Mn, Ni, Zn).

Keywords: Complex, zinc, manganese(II), pyrazine-2-carboxylic acid, structure, thermal stability.

1. Introduction

Pyrazine-2-carboxylic acid (pyzaH) plays an important role in medicine with its antimycobacterial activity. It is formed inside the mycobacterial cells by enzymatic conversion of the prodrug pyrazinamide, which has been used in combination with other antituberculotics for over sixty years.[1,2] The interest and demand of the pharmaceutical industry in tuning the physical and chemical properties of active pharmaceutical ingredients stimulates studies on cocrystals.[3] The possibility of extensive hydrogen bonding makes pyzaH a perfect candidate for the isolation of cocrystals. Two nitrogen and one oxygen atom in the pyzaH molecule act as acceptors of hydrogen bonds and the hydroxyl group acts as a donor of hydrogen bond. Cocrystals of pyzaH with gallic acid[4] or even ternary cocrystals with pyridine-4-carboxamide and pentanedioic acid[3] have been described in the literature.

The ability to ligate and deprotonate the pyzaH molecule is favorable for catalysis. A combination of vanadium compounds and pyzaH, a promoter acid with the advantage of several coordination modes, can provide efficient and versatile catalytic systems for the mild oxidation of alkanes.[5,6]

The proton in the hydroxyl group of pyzaH can be transferred to the nitrogen atom in the zwitterion or easily removed by forming the anion pyza⁻. The observation of coordinated pyzaH as a zwitterion has been documented in complexes of copper(I), $[Cu_2I_2(pyzaH)_2]_n\cdot 3nH_2O$, and bismuth(III), $[Bi(Ph)(pyza)_2(pyzaH)]\cdot H_2O$.[7,8] The anion pyza⁻ enables the crystallization of various salts with organic cations, for example piperazin-1,4-diium, cytosin-3-ium,[4] 4-methyl-1,3-benzothiazol-2(3H)-iminium,[9] phenylmethanaminium,[10] 2-methylpropan-2-aminium[11] or 4-(dimethylamino)pyridin-1-ium.[12] Numerous coordination modes of pyza⁻ have been discovered in hundreds of complex compounds and in many homo- or heterometallic organic frameworks in the Cambridge structural database.[13]

Despite a smaller variety of coordination modes for the molecule than for the anion pyza⁻, four types of pyzaH ligation were found in the complexes (Scheme 1).

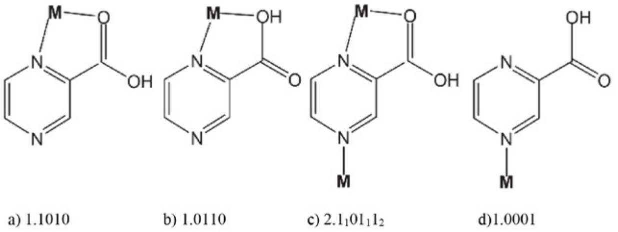

a) 1.1010 b) 1.0110 c) 2.1₁01₁1₂ d)1.0001

Scheme 1. Coordination modes of pyzaH with Harris notation.[14]

The chelate coordination of pyzaH (Scheme 1a), b)) to a single metal ion was found in one cadmium and two copper(II) complexes.[15–17] These complexes are either dinuclear or polymeric with bridging halide or dicyanamide ions. Two bridging chloride ions connect two copper ions in a dinuclear complex $[CuCl_2(pyzaH)_2]_2$.[16] The coordinated O-donor atoms originate from either the carbonyl (Scheme 1a)) or the hydroxyl group (Scheme 1b)) of pyzaH.[16] In the polymeric $[Cu(C_2N_3)_2(pyzaH)_2]_n$, bridging dicyanamide ions link copper ions to form a 2D structure, while bridging iodide ions link cadmium ions in $[CdI_2(pyzaH)_2]_n$ to form 1D chains.[15,17] The chelate coordination mode of pyzaH in both polymeric complexes is presented by Scheme 1a).

A combination of chelating and bridging coordination (Scheme 1c)) of a single pyzaH molecule is present in homometallic and heterometallic polymeric complexes. This coordination mode has been demonstrated in the one-dimensional coordination polymers $[CoBr_2(H_2O)(pyzaH)]_n \cdot nH_2O$[18] and $[Zn_2(H_2O)_4(pyzaH)_2)(SO_4)_2]_n$.[19] Pyrazine-2-carboxylic acid has appeared as an alternative to pyrazine-2,3-dicarboxylic acid in the preparation of metal organic frameworks, which have been the focus of many studies in recent decades. Of particular interest are heterometallic complexes of silver(I) and rhenium(VII) or silver(I) and iron(II) with pyzaH and pyza⁻ as bridging ligands.[20,21] In the search for materials that are efficient in the conversion of solar energy due to their special optical properties and small band gap, oxide-organic hybrid solids of pyzaH, silver(I) and rhenium(VII) have been prepared. The silver ions in $[Ag(pyzaH)(ReO_4)]_n$ are connected by chelate and bridging ligation of pyzaH (Scheme 1c)) and ReO_4^- bridges.[20] In the three-dimensional metal-organic framework $\{[Ag_2Fe_2(MeOH)_2(pyza)_4(pyzaH)](ClO_4)_2\}_n \cdot 3nMeOH$ with interesting catalytic and magnetic properties, pairs of silver(I) ions are connected by molecules of pyzaH (Scheme 1c)), while pyza⁻ links silver(I) to iron(II) and iron(II) to iron(II) ions.[21]

As a monodentate ligand is pyzaH always bonded *via* a nitrogen atom (Scheme 1d)). This type of coordination is characteristic of complexes with metal ions, which act as soft acids.[7,22–25] Copper(I) complexes with monodentate coordination of pyzaH and bridging iodide or chloride ions are 1D polymers.[7,22] In the mononuclear $[HgBr_2(pyzaH)_2]$[25] two molecules of pyzaH are coordinated to mercury(II) as N-donor ligand and in the anions of $[ReX_5(pyzaH)]^-$ only one molecule of pyzaH fulfills the coordination sphere of rhenium(IV).[23,24] Salts containing $[ReX_5(pyzaH)]^-$ have been used as starting compounds for the syntheses of heterometallic compounds with rhenium(IV) and silver(I), which exhibit interesting magnetic properties.

In previous studies, the coordination modes of neutral 3-hydroxypyridin-2-one ($dhpH_2$) and pyridin-2-one (Hhp) with the ions of the first-row transition metals were compared with the binding of the corresponding anions, dhpH⁻ and hp⁻.[26–28] The number of complexes with dhpH⁻ and hp⁻ far exceeds the number of complexes with coordinated molecules. Similarly, complexes with pyza⁻ predominate in the literature, so we decided to focus on the coordination compounds of pyzaH and some transition metals in the fourth period. In contrast to the numerous complexes of pyza⁻ and the first-row transition metal(II) ions[13] only one cobalt(II),[18] one zinc[19] and two copper(II)[16,17] complexes with coordinated pyzaH were characterized by single crystal X-ray diffraction. Chelate coordination of pyzaH (Scheme 1a), b)) was observed in copper(II) complexes and a combination of chelate and bridging ligation (Scheme 1c)) in cobalt(II) and zinc complexes.[16–19] The ability of pyzaH to coordinate to some 3*d* transition metal chlorides was investigated. New complexes of manganese(II), cobalt(II), nickel(II) and zinc were synthesized. We were interested in the coordination mode of pyzaH in the new complexes and in supramolecular aggregations due to hydrogen bonding. The thermal decomposition of the complexes was evaluated and correlated with the structural parameters.

2. Materials and Methods

2. 1. General

Cobalt(II) chloride hexahydrate (Carlo Erba, 98.0%), manganese(II) chloride tetrahydrate (Merck, 99 %), manganese(II) sulfate monohydrate (Sigma Aldrich, 99.0%), nickel chloride (Sigma Aldrich, 97.0%), zinc chloride (Merck, 98%), zinc acetate dihydrate (Johnson Matthey GmbH, 99.5%), pyrazine-2-carboxylic acid (Fluka, 98%) and solvents, methanol, ethanol or acetonitrile, were used as purchased without further purification.

IR spectra (4000–600 cm^{-1}) were acquired using a PerkinElmer Spectrum 100 equipped with a Specac Golden Gate Diamond ATR as a solid sample support.

Elemental analyzes (C, H and N) were performed with a PerkinElmer 2400 Series II CHNS/O microanalyzer at the University of Ljubljana (Department of Organic Chemistry).

Thermal analyzes were performed using a Mettler Toledo TG/DSC 1 instrument (Mettler Toledo, Schwerzenbach, Switzerland) in air at a gas flow of 100 mL/min. The mass of the samples ranged from 7.6 mg to 9.9 mg. The samples in the platinum crucibles were heated from room temperature to 650 °C at a heating rate of 5 °C /min. In each case, the baseline was subtracted.

2. 2. Preparation Procedures

2. 2. 1. Synthesis of $[ZnCl_2(pyzaH)_2] \cdot 2H_2O$ (1)

Method A

The solvent (acetonitrile, 25 mL) was added to pyzaH (0.414 g, 3.34 mmol) and $ZnCl_2$ (0.228 g, 1.67 mmol). The white suspension was stirred in a Schlenk flask with an open side arm at 60 °C for one hour. Crystals **1** grew from the filtrate during slow evaporation of the solvent in six days.

Method B

The solvent (acetonitrile, 25 mL) and the solution of HCl (2.0 mL, 2.0 M) were added to pyzaH (0.414 g, 3.34 mmol) and $Zn(CH_3COO)_2{\cdot}2H_2O$ (0.367 g, 1.67 mmol). The white suspension was stirred in a Schlenk flask with an open side arm at 60 °C for one hour. Crystals **1** grew from the filtrate during slow evaporation of the solvent in four days.

Anal. Calc. Mass fractions of the elements in crystals **1**, w/%, for $C_{10}H_{12}Cl_2N_4O_6Zn$ (M_r = 420.5 g/mol): C, 28.56; H, 2.88; N, 13.32. Found: C, 28.48; H, 2.78; N, 13.02. IR (ATR cm^{-1}) 3456 m, 3346 m, 3082 w, 2429 w, 1895 w, 1698 vs, 1634 w, 1609 m, 1530 w, 1480 w, 1410 m, 1306 vs, 1175 s, 1157 s, 1066 s, 1028 s, 997 m, 983 m, 875 m, 836 m, 777 m, 721 w, 707 m.

2. 2. 2. Synthesis of $[MnCl_2(pyzaH)_2]_n{\cdot}2nH_2O$ (2) and $[MnCl_2(pyzaH)_2]$ (2a)

The solvent (methanol, 25 mL) and a solution of concentrated HCl (2.0 mL) were added to pyzaH (0.414 g, 3.34 mmol) and $MnSO_4{\cdot}H_2O$ (0.282 g, 1.67 mmol). The solution was obtained after four days of stirring at room temperature and then stored in an open beaker. Crystals **2** grew in the solution during evaporation of the solvent. The crystals were unstable outside the solution, only X-ray diffraction analysis was performed.

The solvent (methanol, 25 mL) was added to pyzaH (0.414 g, 3.34 mmol) and $MnCl_2{\cdot}4H_2O$, (0.331 g, 1.67 mmol). The solution obtained after stirring at room temperature for four days was dried *in vacuo* and the non-aquas complex **2a**, $[MnCl_2(pyzaH)_2]$, was gained.

Anal. Calc. Mass fractions of the elements in **2a**, w/%, for $C_{10}H_8Cl_2MnN_4O_4$ (M_r = 374.0 g/mol): C, 32.11; H, 2.16; N, 14.98. Found: C, 32.13; H, 2.20; N, 14.89. IR (ATR cm^{-1}) 3515 bw, 3088 w, 2487 bw, 2156 w, 1720 vs, 1592 w, 1435 m, 1408 m, 1321 vs, 1199 w, 1171 m, 1143 s, 1056 s, 1021 s, 953 w, 869 m, 843 m, 771 s, 734 m.

2. 2. 3. Synthesis of $[CoCl_2(pyzaH)_2]_n{\cdot}2nH_2O$ (3)

The solvent (acetonitrile, 25 mL) and the solution of HCl (2.0 mL, 2.0 M) were added to pyzaH (0.248 g, 2.00 mmol) and $CoCl_2{\cdot}6H_2O$ (0.256 g, 1.08 mmol). The suspension was stirred in a beaker at 70 °C for one hour. Violet crystals **3** grew in the filtrate during evaporation of the solvent in air.

Anal. Calc. Mass fractions of the elements in the crystals **3**, w/%, for $C_{10}H_{12}Cl_2CoN_4O_6$ (M_r = 414.1 g/mol): C, 29.01; H, 2.92; N, 13.53. Found: C, 28.83; H, 2.78; N, 13.12. IR (ATR cm^{-1}) 3511 m, 3366 s, 3086 m, 2500 bw, 1980 bm, 1691 vs, 1596 s, 1525 w, 1479 w, 1455 w, 1401 m, 1308 s, 1175 s, 1156 s, 1060 s, 1028 s, 871 m, 831 m, 776 s, 703 m.

2. 2. 4. Synthesis of $[NiCl_2(pyzaH)_2]$ (4)

The solvent (acetonitrile, 25 mL) and a solution of concentrated HCl (2.0 mL) were added to pyzaH (0.372 g, 3.00 mmol) and $NiCl_2$ (0.194 g, 1.50 mmol). The suspension was stirred in a Schlenk flask at room temperature for five days and then filtered. The non-aquas compound **4**, $[NiCl_2(pyzaH)_2]$, was obtained in the precipitate. When the reaction was repeated at elevated temperature (60 °C, 2 hours), a mixture of $[NiCl_2(pyzaH)_2]$ and $[Ni(pyza)_2]$ was found in the precipitate. No crystals were isolated from the solution of **4** in methanol; when the solvent evaporated a mixture of **4** and $[Ni(pyza)_2]$ was obtained according to the IR spectrum.

Anal. Calc. Mass fractions of the elements in **4**, w/%, for $C_{10}H_8Cl_2N_4NiO_4$ (M_r = 377.8 g/mol): C, 31.79; H, 2.13; N, 14.83. Found: C, 32.07; H, 2.12; N, 14.35. IR (ATR cm^{-1}) 3102 w, 2051 bw, 1721 vs, 1592 w, 1435 m, 1409 m, 1323 vs, 1200 w, 1177 m, 1146 s, 1062 s, 1024 s, 955 w, 866 m, 845 m, 768 s, 735 w.

2. 3. X-ray Structure Determinations

Single crystal X-ray diffraction data were collected on an Agilent SuperNova Dual Source diffractometer with an Atlas detector, using graphite-monochromatized Mo-Kα radiation at 150 K. Data reduction and integration were performed using the CrysAlis PRO software package.[29] Corrections for absorption (multi-scan) were applied in all cases. All structures were solved by direct methods implemented in SIR–2014 or SHELXT and refined by a full–matrix least squares procedure based on F^2 with SHELXL.[30,31] The positions of the hydrogen atoms in pyzaH were unambiguously located from the residual electron density maps for all compounds and the hydrogen atoms in water only in compounds **1** and **2**. Only the positions of the hydrogen atoms in water were refined using O–H distance restraints with $U_{iso}(H) = 1.5U_{eq}(O)$. All other hydrogen atoms were placed at geometrically calculated positions and refined using a riding model. The details of the crystal data collections and the refinement parameters of the complexes **1**–**3** are summarized in Table 1.

The figures depicting the structures were prepared by ORTEP3 and Mercury.[32,33]

X-ray powder diffraction data were collected using a PANalytical X´Pert PRO MPD diffractometer with reflection geometry using Cu-$K_{\alpha1}$ (λ = 1.5406Å) in the 2θ range from 5° to 70° with a step of 0.034° and an integration time of 100 s.

3. Results and Discussion

3. 1. Synthetic Aspects

The syntheses and reaction conditions are shown in Scheme 2.

Table 1. Crystallographic data, data collection and structure refinement data for the compounds **1–3**.

	1	**2**	**3**
Molecular formula	$C_{10}H_{12}Cl_2N_4O_6Zn$	$C_{10}H_{12}Cl_2MnN_4O_6$	$C_{10}H_{12}Cl_2CoN_4O_6$
Color	colorless	colorless	violet
For. mass (g/mol)	420.5	410.07	414.07
Cryst. syst.	monoclinic	monoclinic	monoclinic
Radiation type	Mo *Kα*	Mo *Kα*	Mo *Kα*
Space gr.	$C2/c$ (no. 15)	$P2_1/n$ (no. 14)	$P2_1/n$ (no. 14)
a (Å)	13.2469(6)	6.4539(3)	6.443(2)
b (Å)	5.4354(2)	3.6104(2)	3.5352(5)
c (Å)	21.8060(11)	31.8942(15)	31.379(4)
β (°)	102.365(5)	94.649(4)	95.014(19)
V (Å^3)	1533.66(12)	740.73(3)	712.0(1)
Z (form.)	4	2	2
$D_{cal.}$ (g cm^{-3})	1.82	1.84	1.93
μ (mm^{-1})	1.985	1.288	1.619
Crystal size (mm)	0.3 × 0.2 × 0.2	0.02 × 0.05 × 0.05	0.1 × 0.05 × 0.02
θ Range (°)	3.15–27.5	2.6–30.4	2.61–27.5
Collected refl.	7366	13711	4499
Unique refl.	1756	2074	1650
R_{int}	0.023	0.035	0.084
Observed refl.	1678	1704	1228
No. param.	117	115	107
R^a ($I > 2.0\ \sigma(I)$)	0.0187	0.032	0.0914
wR_2^b	0.0509	0.043	0.198
S	1.07	1.13	1.22
Max/min res. elec. d. (e Å^{-3})	–0.26, 0.41	–0.35, 0.47	–0.60, 1.15

$^a R = \Sigma(|F_o| - |F_c|)/\Sigma|F_o|$, $^b wR_2 = (\Sigma[w(F_o^2 - F_c^2)^2]/\Sigma(wF_o^2)^2)^{1/2.}$

CCDC - 2406449 (**1**), 2406448 (**2**), contain the supplementary crystallographic data for this paper. These data can be obtained free of charge at http://www.ccdc.cam.ac.uk/conts/retrieving.html, or from the Cambridge Crystallographic Data Centre, 12 Union Road, Cambridge CB2 1EZ,UK; Fax: +44-1223-336033; or e-mail: deposit@ccdc.cam.ac.uk.

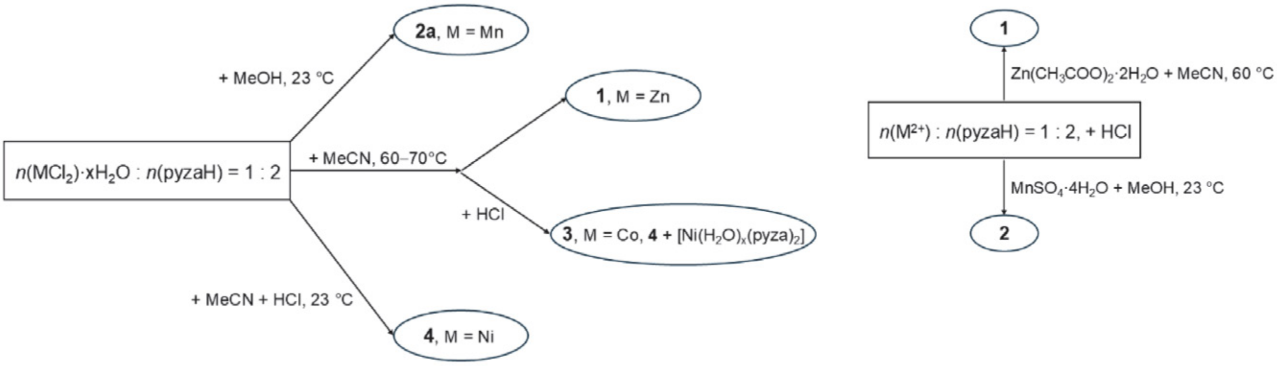

Scheme 2. Syntheses of compounds **1–4** and **2a**.

Complex **1** was crystallized after the reaction of $ZnCl_2$ and pyzaH in acetonitrile or ethanol at elevated temperature. The reaction of $Zn(CH_3COO)_2·2H_2O$ and pyzaH in acetonitrile at 60 °C also resulted in complex **1**, when HCl solution was added. When water was added to the solvent, methanol or ethanol, a deprotonated form of pyzaH and water molecules are coordinated to central zinc ions in the crystals of the known compound $[Zn(H_2O)_2(pyza)_2]$.[34]

All reactions of the manganese(II) salts with pyzaH took place at room temperature. A solution obtained after the reaction of manganese chloride tetrahydrate with pyzaH in methanol was dried *in vacuo*. The powder gained contains $[MnCl_2(pyzaH)_2$, **2a**, according to IR spectrum, X-ray powder diffraction, CHN and thermal analysis. The reaction of $MnSO_4·4H_2O$ and pyzaH in methanol and HCl solution resulted in crystals of **2**. The crystals grew in the solution during evaporation of the solvent from the open beaker.

The addition of HCl solution to a suspension of $CoCl_2·6H_2O$ and pyzaH in acetonitrile at elevated temperature was necessary to isolate complex **3**. In the reactions of $CoCl_2{\cdot}6H_2O$ and pyzaH in a solvent that was a 1:1 mixture of ethanol or acetonitrile and water, a deprotonated form of pyzaH and water molecules are coordinated to central cobalt ions in yellow crystals of the known compound $[Co(H_2O)_2(pyza)_2]$.[34]

In contrast to zinc and manganese chlorides, reactions of cobalt or nickel chlorides and pyzaH only resulted in complexes with ligated pyzaH in the presence of HCl. While the cobalt complex **3** was only isolated after the reaction at elevated temperature, the nickel compound **4** was obtained at room temperature. The reaction of nickel chloride and pyzaH in the presence of HCl at elevated temperature gave a mixture of **4**, $[Ni(H_2O)(pyza)_2]_n$, and $[Ni(H_2O)_2(pyza)_2]$.[34, 35] The dimeric copper complex $[CuCl_2(pyzaH)]_2$ was also prepared only in the presence of HCl at room temperature, similar to nickel complex **4**.[16]

3. 2. IR Spectra

The presence of hydrogen bonded water molecules in the spectra of **1** and **3** was detected by broad bands at 3511 cm^{-1} and 3456 cm^{-1}, whereas these bands are not visible in the spectra of **2a** and **4** (Figures S1–S4).

The typical band for carboxylic acid ν(C=O) appears in pure pyzaH at 1709 cm^{-1}. This band is only slightly shifted in the new complexes **1**–**4**. In aqua zinc and cobalt complexes, **1** and **3**, the band ν(C=O) was observed at 1698 cm^{-1} and 1691 cm^{-1} respectively. The crystal structures of these two compounds confirm a monodentate coordination of pyzaH *via* an N-donor atom. The frequency change is similar to that of the copper(I) compound $[CuCl(pyzaH)_2]_n{\cdot}2nH_2O$ (1690 cm^{-1}) with the same coordination mode of pyzaH. The shift is attributed to different hydrogen bonding in pure and coordinated pyzaH.[22] Oxygen atoms in carbonyl groups are involved as acceptors of hydrogen bonds in **1**, **3** and $[CuCl(pyzaH)_2]_n{\cdot}2nH_2O$, but do not participate in hydrogen bonds connecting pure pyzaH. In contrast, a shift of ν(C=O) to higher wavenumbers was observed in the spectra of non-aquas complexes **2a** (1720 cm^{-1}) and **4** (1721 cm^{-1}). A similar shift to higher wavenumbers was also observed in two ionic rhenium(IV) complexes, $[ReX_5(pyzaH)]^-$ (X = Cl, 1718 cm^{-1}; X = Br, 1730 cm^{-1}) where pyzaH acts as the terminal N-donor ligand.[23,24] The wavenumber indicating ν(C=O) in the spectrum of cocrystals $[MnCl_2(H_2O)_2]_n{\cdot}2nHhp$ (Hhp = pyridin-2-one, 1699 cm^{-1}) is also higher than in pure Hhp (1681 cm^{-1}).[28]

Asymmetric vibrations of carboxylate at much lower frequencies were observed in the complexes with coordinated ion $pyza^-$ instead of the ν(C=O) band at 1710 cm^{-1}.[34] Strong bands for carboxylate vibrations in $[M(H_2O)_2(pyza)_2]$ were observed at 1647 cm^{-1} (M = Zn), 1629 cm^{-1} (M = Mn), 1633 cm^{-1} (M = Co) and 1624 cm^{-1} (M = Ni).[34] The absence of bands for carboxylate vibrations in the new complexes **1**–**4** unambiguously proves coordination of the molecule pyzaH to a central ion in all new compounds.

3. 3. Description of the Structures

3. 3. 1. Crystal structure of $[ZnCl_2(pyzaH)_2]{\cdot}2H_2O$ (1)

Two pyzaH molecules and two chloride ions fulfill coordination sphere of zinc in **1** in a distorted tetrahedral mode (Figure 1a). The asymmetric unit comprises one water molecule and one half of the complex molecule, with the zinc ion lying on a twofold rotation axis. In **1**, pyzaH acts as a monodentate N-donor ligand in contrast to the chelate coordination of pyzaH in $[Zn_2(H_2O)_4(pyzaH)_2)(SO_4)_2]_n$ and in the other complexes of the first row transition metal(II) ions, Co(II) and Cu(II).[16–19] The monodentate coordination via the N-donor atom was also calculated for the isostructural mercury(II) complex $[HgBr_2(pyzaH)_2]{\cdot}2H_2O$ (Figure 1b).[25]

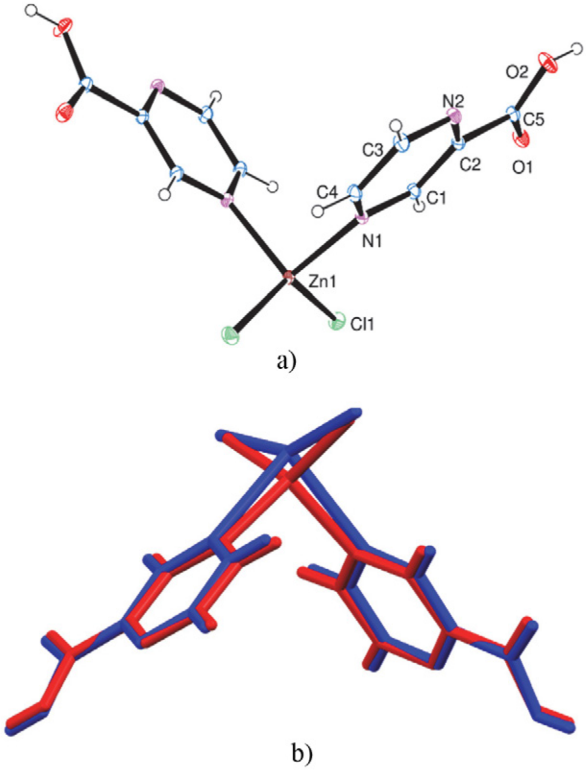

a)

b)

Figure 1. a) ORTEP drawing of $[ZnCl_2(pyzaH)_2]$ (**1**). The atoms are represented by displacement ellipsoids at the 25% probability level. The hydrogen atoms are shown as spheres of arbitrary radius. b) Structure overlay of **1** (red) and $[HgBr_2(pyzaH)_2]$ (blue).

The Zn–N and Zn–Cl bond lengths in **1** are in the same range (Table 1) as in many zinc chloride complexes displaying tetrahedral geometry with monodentate aromatic ligands coordinated *via* an N-donor atom. The ligands in the compared complexes are pyrazine-2-carboxamide, 2-methylpyrazine, 2-aminopyrazine or 2,6-dichloropyrazine.[36–39] Significantly longer bonds were found in a six numbered coordination environment of zinc in $[ZnCl_2(pyza)_2]^{2-}$ (Zn–Cl 2.574(3) Å, Zn–N 2.109(7) Å) or in the homoleptic complex ion $[Zn(pyza)_3]^-$ (Zn–N from 2.153(2) Å to 2.174(2) Å) with chelate coordination of pyrazine-2-carboxylate.[40,41]

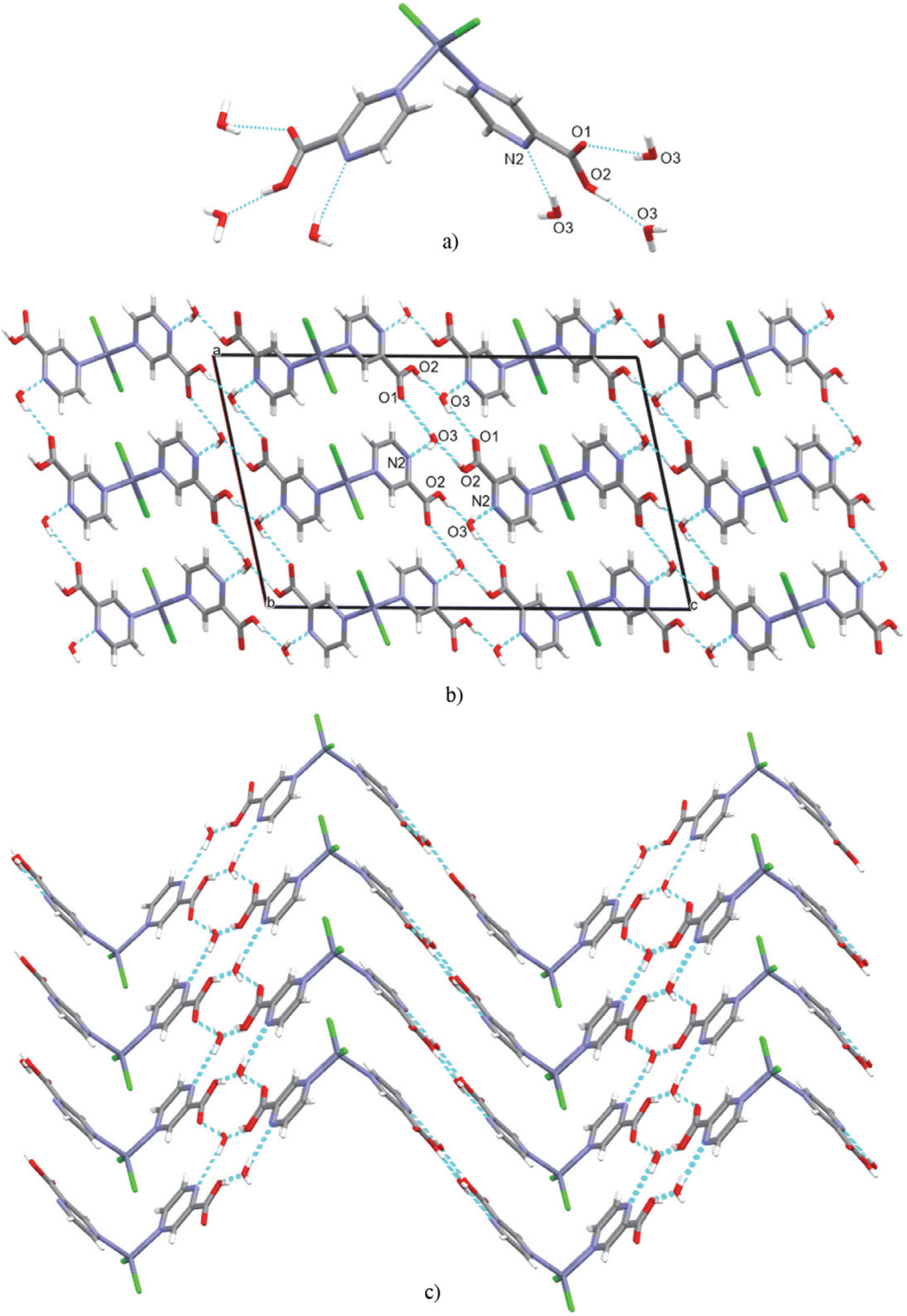

Figure 2. Molecules of **1**. a) Each complex molecule is a donor of two and an acceptor of four hydrogen bonds. b) Complex molecules are connected to water molecules by hydrogen bonds and form wavy layers parallel to the *ac* plane. c) The wavy layers are linked by hydrogen bonds into a 3D structure.

Table 2. Selected geometric parameters (Å, °) in $[ZnCl_2(pyzaH)_2]$ (**1**).

Zn1–Cl1	2.1963(3)	N1–Zn1–N1^i	99.09(6)
Zn1–N1	2.0677(11)	Cl1–Zn1–Cl1^i	126.74(2)
O1–C5	1.2133(17)	Cl1–Zn1–N1	106.01(3)
O2–C5	1.3048(17)	Cl1–Zn1–N1^i	107.81(3)

Symmetry code: (i) 1 – *x*, *y*, ½ – *z*.

A distortion of the tetrahedral angles in **1** is evident in a sharper N1–Zn1–N1^i and a larger Cl1–Zn1–Cl1^i angle (Table 2). A similar deviation was also observed for the angles in tetrahedral zinc chloride complexes with pyrazine-2-carboxamide and 2,6-dichloropyrazine.[36,39] An even stronger distortion of the tetrahedra was detected in the complex of $[HgBr_2(pyzaH)_2]$ due to the steric requirements of the bulkier bromide ions (N1–Hg1–N1^i 86.9(6)°, Br1–Hg1–Br1^i 153.72(12)°).[25] Consequently, the dihedral angle between the planes through organic ligands is larger in **1** (84.27(11)°) than in $[HgBr_2(pyzaH)_2]$ (78.4(9)°). On the other hand, a less pronounced distortion of the tetrahedra was observed in some $[ZnCl_2L_2]$ (L = 2-aminopyrazine, apyz, or 2-methylpyrazine, mpyz). In $[ZnCl_2(apyz)_2]$, the Cl–Zn–Cl (114.58(2)°) angle is sharper and the N–Zn–N (106.52(7)°) angle is wider than in **1**.[38] In $[ZnCl_2(mpyz)_2]$, only a wider Cl–Zn–Cl angle (125.41(4)°or 128.26(4)°) differs significantly from the tetrahedral angle.[37]

All good hydrogen bond donors, OH in water and the hydroxyl group of pyzaH are engaged in hydrogen bonding in **1**, the acceptors are uncoordinated nitrogen atoms and carbonyl oxygen atoms in the molecules of pyzaH (Table 3) and oxygen atoms in water.

Table 3. Hydrogen bonds (Å, °) for $[ZnCl_2(pyzaH)_2]$ (**1**).

D–H····A	**D–H**	**H····A**	**D····A**	**D–H····A**
O2–H11····O3^{ii}	0.83(2)	1.71(3)	2.523(2)	169(3)
O3–H31····O1^{iii}	0.76(2)	2.07(2)	2.7992(2)	161(2)
O3–H32····N2^{iv}	0.81(3)	2.07(3)	2.864(2)	166(2)

Symmetry code: (ii) 1 – *x*, –*y*, 1 – *z*; (iii) ½ + *x*, 3/2 + *y*, *z*, (iv) *x*, 2 + *y*, *z*.

Each complex molecule forms altogether six hydrogen bonds with six water molecules (Figure 2 a). Solvate molecules of water are involved as donors (O3–H31····O1^{iii}, O3–H32····N2^{iv}) and acceptors (O2–H11····O3^{ii}) of hydrogen bonds creating $R_4^4(12)$ and $R_4^4(14)$ bonding motifs (Figure 2 b). Many donor and acceptor groups involved in intermolecular hydrogen bonding enable construction of a 3D structure (Figure 2 b), c)).

3. 3. 2. Crystal structure of 2, $[MnCl_2(pyzaH)_2]_n \cdot 2nH_2O$ and 3, $[CoCl_2(pyzaH)_2]_n \cdot 2nH_2O$

Complexes **2** and **3** are isostructural (Figure 3 a)); the manganese(II) chloride complex with pyzaH is depicted in Figure 3 b). The crystal structure was perfectly refined only for **2**, while the poor quality of crystals **3** resulted in a less accurate refinement of the crystal structure.

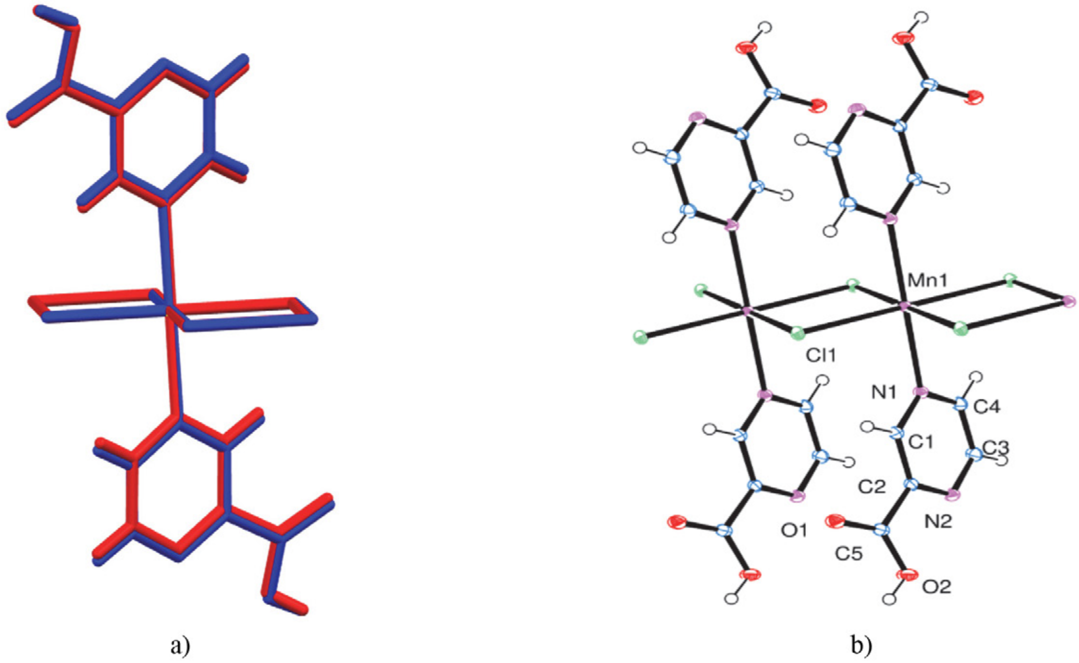

Figure 3. a) Structure overlay of $[MnCl_2(pyzaH)_2]_n \cdot 2nH_2O$ (**2** blue) and $[CoCl_2(pyzaH)_2]_n \cdot 2nH_2O$ (**3** red). b) ORTEP drawing of $[MnCl_2(pyzaH)_2]_n \cdot 2nH_2O$ (**2**). The atoms are represented by displacement ellipsoids at the 25% probability level. The hydrogen atoms are shown as spheres of arbitrary radius.

Four chloride ions and two nitrogen atoms of pyzaH in *trans* positions are coordinated to each metal(II) ion in **2** and **3** in an octahedral mode. An edge sharing of octahedra results in linear chains with double chloride bridges connecting the metal(II) ions in a 1D coordination polymer. The chains are parallel to the *b* axis. All M_2Cl_2 rings in the chains of **2** and **3** are coplanar due to the monodentate N-donor ligands in *trans* positions (Figure 4). Similar neutral manganese(II) polymer chains with coplanar Mn_2Cl_2 rings are found in only a few structures, for example, in cocrystals of $[MnCl_2(H_2O)_2]_n$ and pyridin-2-one (Hhp) or 4-aminopyridinium chloride (apyCl).[28,42] N-donor ligands are usually coordinated in *cis* positions to manganese(II) in $[MnCl_2]_n$ chains, leading to the formation of zigzag chains as in $[MnCl_2(maepy)]_n$ (maepy = (methylamino)ethylpyridine).[43] The adjacent Mn_2Cl_2 rings in $[MnCl_2(maepy)]_n$ are almost perpendicular with a dihedral angle of 84.58°. Planar Mn_2Cl_2 rings were also found in a complex of pyza$^-$, $[MnCl(H_2O)(pyza)]_n$. In this complex, linear chains of manganese(II) ions linked by bridging pyza$^-$ are connected in a 2D structure by double chloride bridges forming isolated Mn_2Cl_2 rings.[44]

The close proximity of the pyrazine rings within the same chain enables an off-center parallel stacking arrangement of the coordinated pyzaH molecules in **2** (Figure 4).[45] The relevant parameters of this interaction in **2** are: centroid–centroid distance 3.610(1) Å, interplanar distance 3.414(1) Å, dihedral angle 0° and offset angle 19.0°. As a consequence of the interactions between parallel coordinated pyzaH molecules the bond lengths Mn–Cl and Mn····Mn distances in **2** (Table 4) are shorter than in compounds with similar chains of coplanar Mn_2Cl_2 rings. In cocrystals of $[MnCl_2(H_2O)_2]_n$ or in the complex $[MnCl_2(maepy)]_n$, Mn–Cl bonds are approximately 0.10 Å longer and Mn····Mn distances from 0.15 Å to 0.33 Å longer.[28, 42, 43] Mn····Mn distances in **2** are also shorter than in $[MnCl(H_2O)(pyza)]_n$ (3.664(4) Å).[44] Mn–N bond lengths in **2** and in $[MnCl_2(maepy)]_n$ (2.303(1) Å) are in the same range.[43]

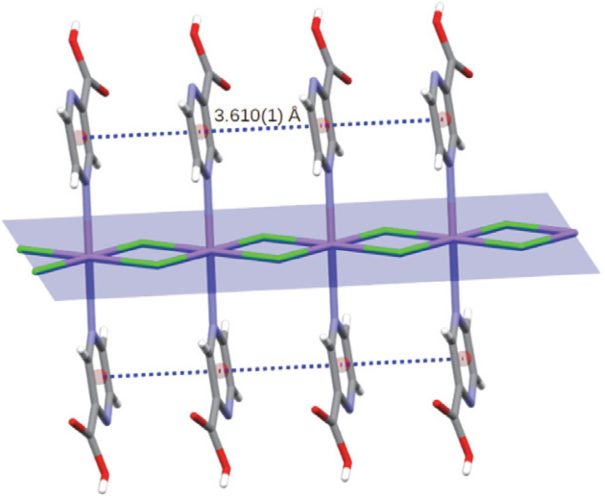

Figure 4. Coplanar Mn_2Cl_2 rings and an off-center parallel stacking arrangement of the coordinated pyzaH molecules in **2**.

As far as we know 1D polymers of cobalt ions connected solely by double chloride bridges have only been described in cocrystals of $[CoCl_2(H_2O)_2]_n$ and Me_3NHCl.[46] Chains of cobalt ions are also characteristic of $[Co_2Cl_4(diglyme)]_n$ (diglyme = di(2-methoxyethyl) ether) with octahedrally and tetrahedrally coordinated cobalt ions connected by single and double chloride bridges.[47] Similar to **2**, the interactions between pyrazine rings in **3** result in shorter Co····Co distances (Table 4) than in $[CoCl_2(H_2O)_2]_n$ (3.637(3) Å), while in $[Co_2Cl_4(diglyme)]_n$ a shorter and a longer Co····Co distance corresponding to one (4.306(1) Å) or two (3.124(1) Å, 3.436(1) Å) bridging chloride ions connecting adjacent cobalt(II) ions were calculated.[46,47]

Table 4. Selected geometric parameters (Å, °) in $[MnCl_2(pyzaH)_2]_n\cdot 2nH_2O$ (**2**) and $[CoCl_2(pyzaH)_2]_n\cdot 2nH_2O$ (**3**).

Mn1–Cl1	2.4990(5)	Co1–Cl1	2.416(2)
Mn1–Cl1^{i}	2.5134(5)	Co1–Cl1^{i}	2.454(2)
Mn1–N1	2.3021(13)	Co1–N1	2.165(6)
O1–C5	1.216(2)	O1–C5	1.215(10)
O2–C5	1.298(2)	O2–C5	1.298(8)
Mn1…Mn1^{i}	3.6104(2)	Co1…Co1^{i}	3.535(1)
Cl1–Mn1–N1	88.52(4)	Cl1–Co1–N1	88.57(18)
Cl1^{i}–Mn1–N1	88.12(4)	Cl1^{i}–Co1–N1	89.40(18)
Cl1–Mn1–Cl1^{i}	92.16(1)	Cl1–Co1–Cl1^{i}	93.07(7)
Cl1–Mn1–Cl1^{ii}	87.85(1)	Cl1–Co1–Cl1^{ii}	86.93(7)

Symmetry code: (i) x, $1 + y$, z; (ii) (ii) $-x$, $-1 - y$, $-z$.

All good hydrogen bond donors and acceptors are involved in hydrogen bonding. Each coordinated pyzaH is a donor of one (O2–H2····O3) and an acceptor of two (O3–H31····N2^{iii}, O3–H32····O1^{iv}) hydrogen bonds involving three water molecules (Figure 5 a), Table 5). Infinite $[MnCl_2(pyzaH)_2]_n$ chains are connected to the 3D structure by hydrogen bonds engaging water molecules (Figure 5 b)).

Table 5. Hydrogen bonds (Å, °) in $[MnCl_2(pyzaH)_2]_n\cdot 2nH_2O$ (**2**).

D–H····A	*D*–H	H····A	*D*····A	*D*–H····A
O2–H2····O3	0.840	1.690	2.523(2)	174.0
O3–H31····N2^{iii}	0.83(3)	2.07(3)	2.895(2)	171(3)
O3–H32····O1^{iv}	0.82(3)	2.19(3)	2.971(2)	159(3)

Symmetry code: (iii) $½ - x$, $-½ + y$, $½ - z$; (iv) $-½ - x$, $½ + y$, $½ - z$.

3. 3. 3. X-ray Powder Diffraction Analysis

The results of the X-ray powder diffraction analysis confirm the isostructural nature of complexes **2a** and **4** (Figure 6). Minor differences in the unit cell dimensions are expected due to a larger Mn^{2+} (83 pm) and a smaller Ni^{2+} (69 pm) ion in complexes **2a** and **4**. Due to the larger unit cell of complex **2a**, the diffraction peaks of this complex are at lower 2θ values than the peaks for complex **4**. The shift of the diffraction peaks of the compared

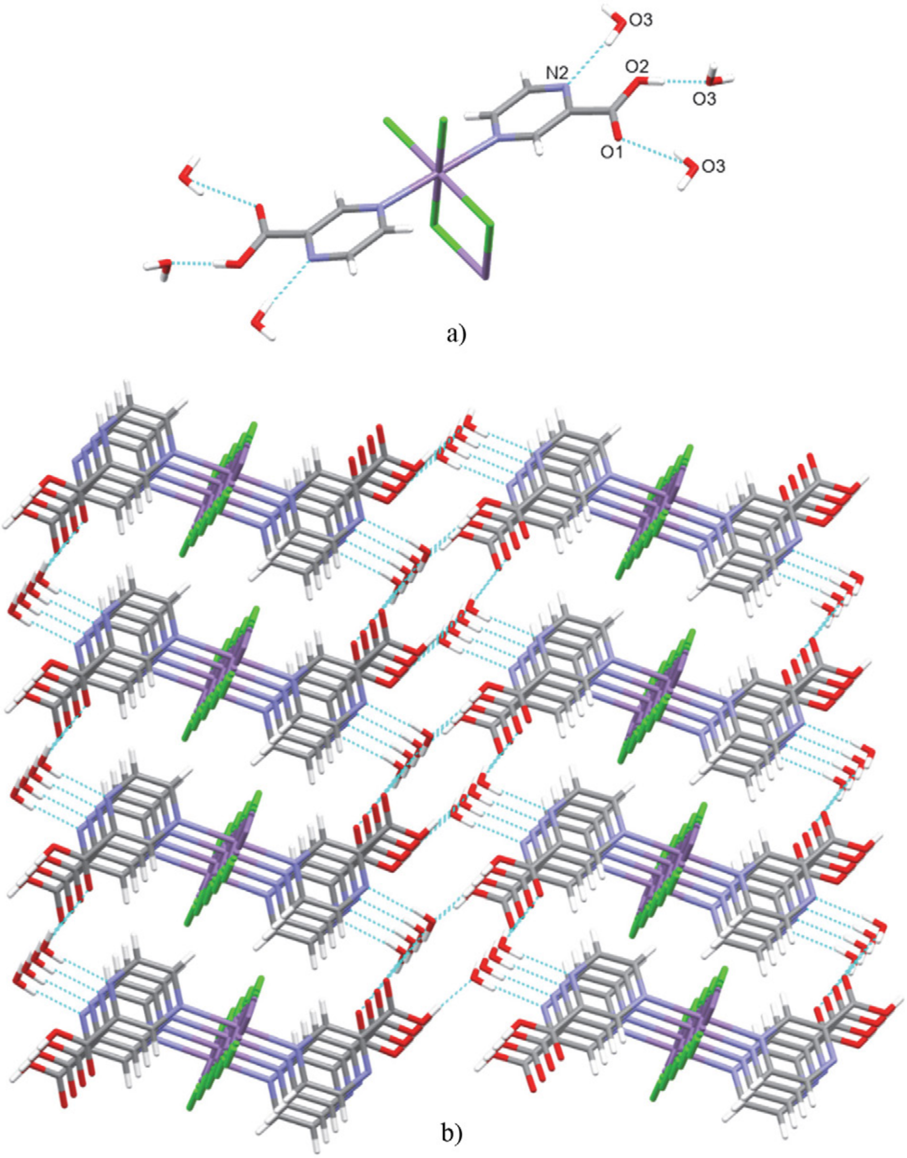

Figure 5. a) Each coordinated pyzaH molecule in complex **2** is a donor of one and an acceptor of two hydrogen bonds. b) The chains of [Mn-$Cl_2(pyzaH)_2]_n$ are connected to water molecules by hydrogen bonds and form the 3D structure.

complexes is negligible at lower 2θ values, but increases at higher angles.

As expected, the calculated X-ray diffraction powder pattern of **2** differs from the one measured for **2a** (Figure S5).

3. 4. Thermal Analysis

The result of the thermal analysis of complex **1** is depicted in Figure 7. Water molecules that are not coordinated to zinc ions evaporate between 110 °C and 160 °C in the first decomposition step. The mass loss in this step (8.6%) corresponds to exactly two moles of water per one mole of compound **1** (8.6%). The decomposition continues in several poorly resolved steps up to a temperature of 585 °C. The reactions are endothermic, with the exception of the last reaction, the formation of zinc oxide in air, which is exothermic. The total mass loss observed during the analysis is higher (86 %) than expected for the conversion of $[ZnCl_2(pyzaH)_2]\cdot 2H_2O$ to ZnO (80.6%), probably due to the evaporation of some zinc prior to oxidation.

Complex **1** is thermally less stable than pure pyrazine-2-carboxylic acid, which decomposes completely in air in the temperature range between 170 °C and 220 °C.[34] In contrast to pyzaH, the decomposition of **1** is completed at a higher temperature (585 °C). A comparison of the thermal analysis of **1** and the zinc complex with pyrazine-2-carboxylate, $[Zn(H_2O)_2(pyza)_2]$ in air, shows some important differences.[34] The loss of water occurs in $[Zn(H_2O)_2(pyza)_2]$ at a higher temperature (170 °C) in a

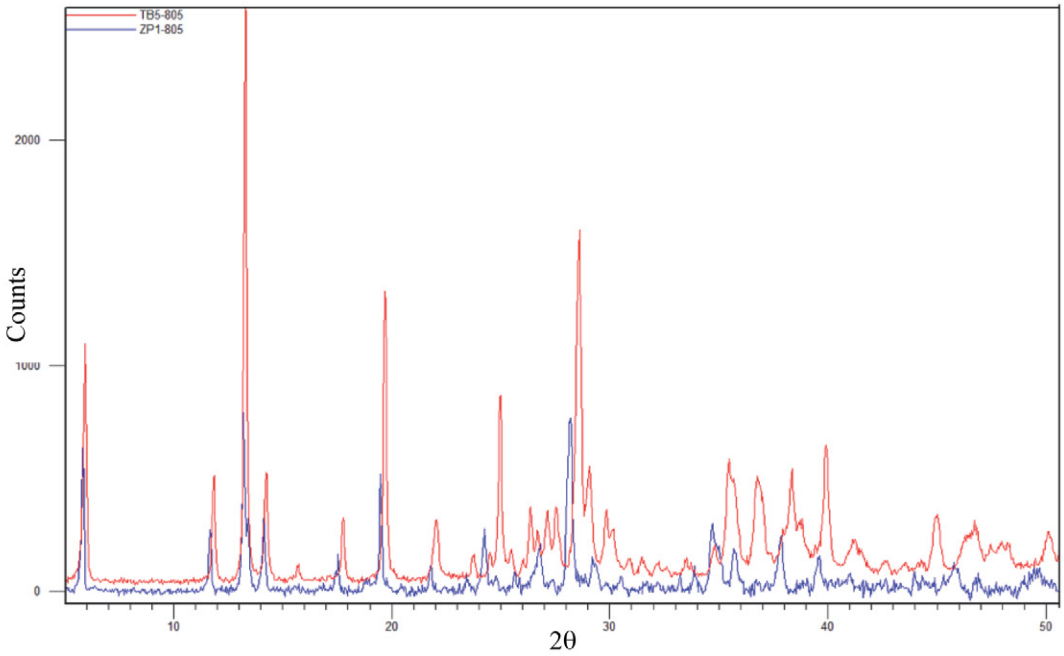

Figure 6. Measured X-ray powder diffractograms for **2a** (in blue) and **4** (in red).

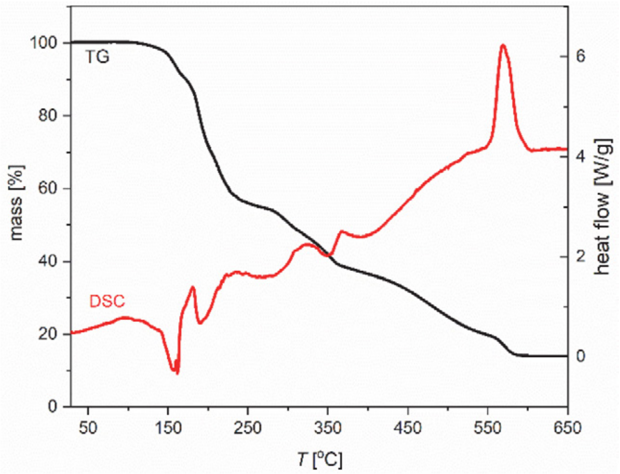

Figure 7. Thermal analysis of $[ZnCl_2(pyzaH)_2]\cdot 2H_2O$ (**1**).

well-defined first step, which is due to the coordination of water to the zinc ion in the complex. While the decomposition of **1** immediately follows dehydration at 170 °C, the second decomposition step of $[Zn(H_2O)_2(pyza)_2]$ does not begin until 280 °C. The lower thermal stability of **1** compared to $[Zn(H_2O)_2(pyza)_2]$ is explained by the monodentate coordination of pyzaH in **1** and the chelate ligation of $pyza^-$ in $[Zn(H_2O)_2(pyza)_2]$. The thermal decomposition of both **1** and $[Zn(H_2O)_2(pyza)_2]$ is completed at 585 °C with the formation of ZnO.

The results of the thermal analysis confirm the isostructural nature of complexes **2a** and **4** (Figure 8). Both compounds decompose in air in two steps, with the first step starting at temperatures above 170 °C and the second one above 300 °C. Thermal stability up to 170 °C indicates anhydrous complexes of manganese(II), **2a**, and nickel, **4**. The thermal decomposition of complex **4** is completed at 510 °C and of complex **2a** at 530 °C with the formation of metal(II) oxides. The total mass loss observed for **2a** (81.1 %) and **4** (83 %) at 520 °C agrees well with the calculated mass loss for the conversion of $[MCl_2(pyzaH)_2]$ to MO (M = Mn, 81 %; Ni, 80.2 %). The last step of the decomposition is strongly exothermic, which indicates the formation of metal(II) oxides in air. The oxidation of MnO takes place above 590 °C as shown by the mass gain (Figure 8).

The thermal decomposition of the complexes with pyrazine-2-carboxylate, $[M(H_2O)_2(pyza)_2]$ (M = Mn, Ni), is also a two-step process.[34] In the first step, in the temperature range between 150 °C and 170 °C, a minor mass loss (≈10 %) due to coordinated water is observed. The rest of the mass loss occurs in the second step above 360 °C giving MO. The decomposition of $[M(H_2O)_2(pyza)_2]$ (M = Mn, Ni) is completed at a lower temperature (420 °C) than the decomposition of **2a** and **4** (530 °C and 510 °C).

4. Conclusions

The new manganese(II), cobalt(II), nickel(II) and zinc complexes with pyzaH were prepared from the corresponding chlorides and pyzaH under mild conditions at room temperature or in moderately heated solutions in open Schlenk flasks. The isolation of the cobalt (**3**) and nickel (**4**) complexes required the addition of hydrochloric acid. The manganese(II) (**2**) and zinc (**1**) chloride complexes with pyzaH were also prepared from the corresponding sulfate or acetate in the presence of HCl.

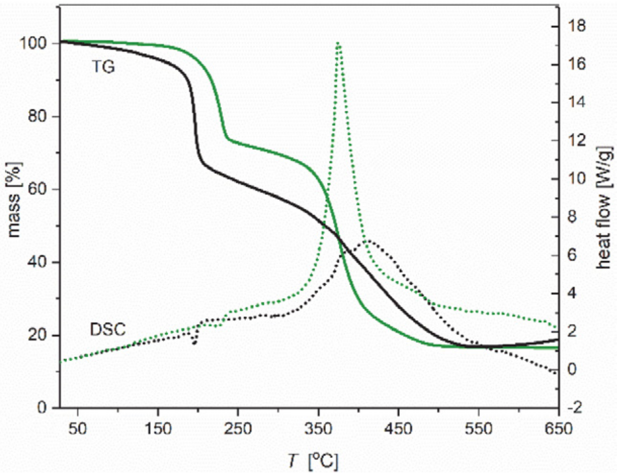

Figure 8. Thermal analysis of **2a** (black lines) and **4** (green lines).

The results of X-ray diffraction analysis revealed the mononuclear nature of complex **1** and polymeric chains in complexes **2** and **3**. This confirms that tetrahedral complexes are more readily formed with Zn^{2+} than with cations of other *d*-block elements. The preference of Zn^{2+} ions to form tetrahedral complexes resulted in mononuclear Zn^{2+} complex in contrast to 1D polymers in **2** and **3** with octahedral coordination of Mn^{2+} and Co^{2+}. The coordination of pyzaH as a terminal N-donor ligand was previously found only in compounds with metal ions characterized as soft acids. In our study, the same monodentate coordination of pyzaH was found in all three complexes, including complex **2** with Mn(II), which is considered a hard acid. The M_2Cl_2 rings forming chains in **2** and **3** are coplanar due to the *trans* coordinated pyzaH molecules. The proximity of the pyrazine rings within the same chain allows an off-center parallel stacking arrangement of the coordinated pyzaH molecules in **2** and **3**. The hydrogen bonds between the water molecules and the coordinated pyzaH molecules in **1**, **2** and **3** lead to 3D structures.

The thermal stability of the complex **1** with monodentate coordination of pyzaH is lower than the thermal stability of $[Zn(H_2O)_2(pyza)_2]$ with chelate ligation of $pyza^-$. During the thermal decomposition of **1**, **2a** and **4** in air, oxides MO (M = Mn, Ni, Zn) are formed.

Acknowledgments and founding

The author would like to thank the students Tina Boh, Klara Derganc, Natlija Papež and Žiga Počervina for their help with the syntheses and the colleagues Romana Cerc Korošec and Damjan Erčulj for the thermogravimetric measurements.

The author acknowledges the support of the Center for Research Infrastructure at the University of Ljubljana, Faculty of Chemistry and Chemical Technology, which is part of the Network of Research and Infrastructural Centres UL (MRIC UL) and is financially supported by the Slovenian Research Agency (Infrastructure program No. I0-0022).

This research was funded by the Slovenian Research Agency (Grant no. P1-0230-0175).

5. References

1. P. Singh, A. K. Mishra, S. K. Malonia, D. S. Chauhan, V. D. Sharma, K. Venkatesan, V. M. Katoch, *J. Commun. Dis.* **2006**, *38*, 288–298. **DOI:**10.1016/j.dld.2006.01.026
2. M. Stehr, A. A. Elamin, M. Singh, *Curr. Top. Med. Chem.* **2014**, *14*, 110–129. **DOI:**10.2174/1568026613666131113152908
3. H. Kulla, A. A. L.Michalchuk, F. Emmerling, *Chem. Commun.* **2019**, *55*, 9793–9796. **DOI:**10.1039/C9CC03034D
4. K. D. Prasad, S. Cherukuvada, R. Ganduri, L. D. Stephen, S. Perumalla, T. N. G. Row, *Cryst. Growth Des.* **2015**, *15*, 858–866. **DOI:**10.1021/cg501642m
5. A. M. Kirillova, G. B. Shul'pinb, *Coordin. Chem. Rev.* **2013**, *257*, 732–754. **DOI:**10.1016/j.ccr.2012.09.012
6. M. Sutradhar, L. M. Martins, M. F. C. G. da Silvaa, A. J. L. Pombeiroa, *Coordin. Chem. Rev.* **2015**, *301–302*, 200–239. **DOI:**10.1016/j.ccr.2015.01.020
7. M. A. S. Goher, T. C. W. Mak, *Polyhedron* **1995**, *14*, 2587–2594. **DOI:**10.1016/0277-5387(94)00489-2
8. O. Anjaneyulu, D. Maddileti, K. C. K. Swamy, *Dalton Trans.* **2012**, *41*,1004–1012. **DOI:**10.1039/C1DT11207D
9. S. Li, K. Hu, X. Gao, S. Jin, B. Chen, Z. Chen, L. He, D. Wang, *J. Mol. Struct.* **2022**, *1261*, 132770. **DOI:**10.1016/j.molstruc.2022.132770
10. W. Xu, K. Hu, Y. Lu, H. Ye, S. Jin, M. Li, M. Guo, D. Wang, *J. Mol. Struct.* **2020**, *1219*, 128554. **DOI:**10.1016/j.molstruc.2020.128554
11. X. Yang, Y. Zhu, X. Chen, X. Gao, S. Jin, B. Liu, L. He, B. Chen, D. Wang, *J. Mol. Struct.* **2021**, *1251* **DOI:***10.1016/j.molstruc.2021.131917*
12. W. Fang, B. Chen, D. Chen, S. Wang, Y. Yan, S. Jin, W. Xu, D. Wang, *J. Mol. Struct.* **2020**, *1203*, 127353. **DOI:**10.1016/j.molstruc.2019.127353
13. See the Cambridge Structural Database (CSD, version June 2024): C. R. Groom, I. J. Bruno, M. P. Lightfoot and S. C. Ward, *Acta Cryst.* **2016**, *B72*, 171–179. **DOI:**10.1107/S2052520616003954
14. R. A. Coxall, S. G. Harris, D. K. Henderson, S. Parsons, P. A. Tasker, R. E. P. Winpenny, *J. Chem. Soc., Dalton Trans.* **2000**, 2349–2356. **DOI:**10.1039/b001404o
15. D. M. Ciurtin, M. D. Smith, H. C. zur Loye, *Polyhedron* **2003**, *22*, 3043–3049. **DOI:**10.1016/S0277-5387(03)00430-3
16. C. L. Klein, L. M. Trefonas, C. J. O'Connor, R. J. Majeste, *Cryst. Struct. Commun.* **1981**, *10*, 891–894.
17. S. Konar, U. Saha, M. Dolai, S. Chatterjee, *J. Mol. Struct.* **2014**, *1075*, 286–291. **DOI:**10.1016/j.molstruc.2014.06.080
18. C. Dares, R. Fournier, A. B. P. Lever, *Acta Crystallogr. E* **2011**, *67*, m1798–m1799. **DOI:**10.1107/S1600536811048628
19. X. H. Zhao, *Russ. J. Coord. Chem.* **2011**, *37*, 585–588.

DOI:10.1134/S1070328411080124

20. H. Lin, X. Wu, P. A. Maggard, *Inorg. Chem.* **2009**, *48*, 11265–11276. **DOI:**10.1021/ic901749r
21. S. Nayak, K. Harms, S. Dehnen, *Inorg. Chem*. **2011**, *50*, 2714–2716. **DOI:**10.1021/ic1019636
22. M. A. S. Goher, F. A. Mautner, R. Vicente, *J. Mol. Struct.* **2007**, *846,* 28–33. **DOI:**10.1016/j.molstruc.2007.01.016
23. L. Arizaga, R. Gonzalez, D. Armentano, G. De Munno, M. A. Novak, F. Lloret, M. Julve, C. Kremer, R. Chiozzone, *Eur. J. Inorg. Chem*. **2016**, 1835–1845. **DOI:**10.1002/ejic.201501487
24. A. Cuevas, C. Kremer, M. Hummert, H. Schumann, F. Lloret, M. Julve, J. Faus, *Dalton Trans.* **2007**, 342–350. **DOI:**10.1039/B611888G
25. G. W. Wang, W. Y. Wu, L. H. Zhuang, J. T. Wang, *Acta Crystallogr., Sect.E: Struct. Rep. Online* **2008**, *64*, m13. **DOI:**10.1107/S1600536807061491
26. S. Petriček, *Polyhedron* **2019**, *167*, 11–25. **DOI:**10.1016/j.poly.2019.03.050
27. S. Petriček, *Molecules* **2020**, *25*, 846–869. **DOI:**10.3390/molecules25040846
28. S. Petriček, *J. Mol. Struct.* **2022**, *1260*, 132790. **DOI:**10.1016/j.molstruc.2022.132790
29. CrysAlisPro, version 1.171.43.121a; Rigaku Oxford Diffraction: Yarnton, UK, 2024.
30. M. C. Burla, R. Caliandro, B. Carrozzini, G. L. Cascarano, C. Cuocci, C. Giacovazzo, M. Mallamo, A. Mazzone, G. Polidori, *J. Appl. Cryst.* **2015**, *48*, 306–309. **DOI:**10.1107/S1600576715001132
31. G. M. Sheldrick, *Acta Crystallogr*. **2015**, *C71*, 3–8. **DOI:**10.1107/S2053229614024218
32. J. J. Farrugia, *J. Appl. Cryst.* **1997**, *30*, 565. **DOI:**10.1107/S0021889897003117
33. C. F. Macrae, I. Sovago, S. J. Cottrell, P. T. A. Galek, P. McCabe, E. Pidcock, M. Platings, G. P. Shields, J. S. Stevens, M. Towler and P. A. Wood, *J. Appl. Cryst*. **2020**, *53*, 226–235. **DOI:**10.1107/S1600576719014092
34. G. Świderski, S. Wojtulewski, M. Kalinowska, R. . Świsłocka, A. Z. Wilczewska, A. Pietryczuk, A. Cudowski, W. Lewandowski, *Polyhedron* **2020**, *175*, 114173. **DOI:**10.1016/j.poly.2019.114173
35. M. Shahwaz Ahmad, M. Khalid, M. Shahnawaz Khan, M. Shahid, M. Ahmad, *Cryst. Eng. Comm.* **2021**, *23*, 6253–6266. **DOI:**10.1039/D1CE00815C
36. S. A. Shirvan, S. H. Dezfuli, *Acta Crystallogr., Sect.E: Struct. Rep. Online* **2012**, *68*, m546. **DOI:**10.1107/S1600536812013888
37. C. Nather, I. Jess, S. Mangelsen, *Z. Naturforsch., B. Chem. Sci.* **2023**, *78*, 113−120. **DOI:**10.1515/znb-2022-0306
38. S. Gao, S. W. Ng, *Acta Crystallogr., Sect.E: Struct. Rep.Online* **2011**, *67*, m1049−m1050. **DOI:**10.1107/S1600536811026031
39. C. Hu, U. Englert, *Acta Cryst.* **2001**, *C57*, 1251−1252. **DOI:**10.1107/S0108270101012136
40. H. R. Khavasi, A. Gholami, M. Hosseini, L. Nikpoor, K. Eskandari, *Cryst. Growth Des.* **2020**, *20*, 2266−2274. **DOI:**10.1021/acs.cgd.9b01385
41. N. Podjed, B. Modec, *J. Mol. Struct.* **2023**, *1284*, 135457. **DOI:**10.1016/j.molstruc.2023.135457
42. D. Zaouali Zgolli, H. Boughzala, A. Driss, *Acta Crystallogr.* **2009**, *E65*, m921. **DOI:**10.1107/S1600536809026804
43. D. Domide, O. Hübner, S. Behrens, O. Walter, H. Wadepohl, E. Kaifer, H. J. Himmel, *Eur. J. Inorg. Chem*. **2011**, 1387–1394. **DOI:**10.1002/ejic.201100019
44. D. Huang, X. Zhang, C. Chen, F. Chen, Q. Liu, D. Liao, L. Li, L. Sun, *Inorg. Chim. Acta* **2003**, *353*, 284–291. **DOI:**10.1016/S0020-1693(03)00325-6
45. C. Janiak, *J. Chem. Soc. Dalton Trans.* **2000**, 3885–3896. **DOI:**10.1039/b003010o
46. D. B. Losee, J. N. McElearney, G. E. Shankle, R. L. Carlin, *Phys. Rev. B* **1973**, *8,* 2185–2196. **DOI:**10.1103/PhysRevB.8.2185
47. S. Petriček, *Croat. Chem. Acta* **2011**, *84*, 515–520. **DOI:**10.5562/cca1747

Povzetek

Sintetizirali smo nove koordinacijske spojine cinkovega (**1**), manganovega(II) (**2** in **2a**), kobaltovega(II) (**3**) in nikljevega(II) klorida (**4**) s pyzaH (pirazin-2-karboksilna kislina). Rezultati rentgenske strukturne analize potrjujejo, da se molekule pyzaH koordinirajo v spojinah **1**, **2** in **3** kot enovezni ligandi prek obročnega dušikovega atoma. Kloridni ioni so vezani kot terminalni ligandi v enojedrni spojini **1**, $[ZnCl_2(pyzaH)_2]\cdot 2H_2O$, oziroma kot mostovni ligandi v 1D kompleksih $[MCl_2(pyzaH)_2]_n\cdot 2nH_2O$ (M = Mn, **2**, Co, **3**). Razlike v vezavi kloridnih ionov, interakcijah med vezanimi molekulami pyzaH in vodikovih vezeh v izoliranih spojinah omogočajo različno povezavo gradnikov v snovi. V nasprotju s kristali izoliranimi za spojine **1**, **2** in **3** v spojinah mangana(II) (**2a**) in niklja(II) (**4**) ni vezana voda. Za spojini **2a** in **4** lahko glede na IR spektre in rezultate termične analize predpostavimo formulo $[MCl_2(pyzaH)_2]$. Rezultati rentgenske praškovne analize in termične analize potrjujejo, da sta spojini **2a** in **4** izostrukturni. Monodentatna vezava molekul pyzaH v **1** je vzrok za nizko termično stabilnost kompleksa **1**. Po termičnem razpadu spojin **1**, **2a** in **4** v zraku nastanejo MO (M = Mn, Ni, Zn).